Laser Ablation Powered Mini-Thruster

Claude R. Phipps[*a], James R. Luke[**b], Glen G. McDuff[b], Thomas Lippert[c]
[a]Photonic Associates; [b]NMT/Institute for Engineering Research and Applications
[c]Paul Scherrer Institut

ABSTRACT

We have developed a new type of miniature jet for pointing microsatellites. It is based on laser ablation produced by a multi-mode diode laser. The target is a specially prepared tape with a transparent layer through which the laser light passes and an absorbing layer which produces the thrust. We have achieved specific impulse up to 1000 seconds (greater than possible with chemistry), together with laser momentum coupling coefficients of order 6 dyne/W. The preprototype should achieve 100 dynes of thrust. We will discuss the target interaction physics, the materials science involved in creating the targets, and some of our measurements with the preprototype thruster.

1. INTRODUCTION

Unknown as a field prior to 1972 [1], laser ablation propulsion is now progressing rapidly. One of the latest innovations is the micro laser plasma thruster (μLPT). The micro-Laser Plasma Thruster (μLPT) is a sub-kg micropropulsion option which is intended for attitude control and stationkeeping on microsatellite platforms. A lens focuses a laser diode beam on the ablation target, producing a miniature jet that provides the thrust. The conceptual basis for this thruster was reported earlier in the HPLA symposium series [2]. Single impulse dynamic range is nearly 5 orders of magnitude, and the minimum impulse bit is 1 nano N-s in a 100μs pulse. The diode is a low-voltage device with electrical efficiency in excess of 50%. [Phipps and Luke 2002]. The μLPT is an alternative technology to the micro pulsed plasma thruster (μPPT) for micro- and nano-satellite microthrusters.

In this paper, we will emphasize the theoretical aspects of laser micropropulsion, and the companion paper[3] will discuss device development and the results of our continuous thrust experiments.

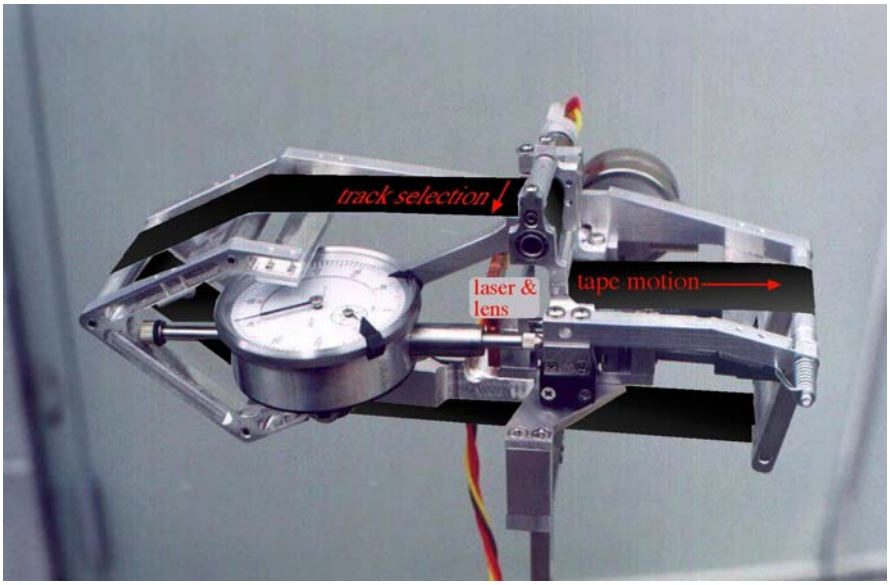

Figure 1. Preprototype micro Laser Plasma Thruster (gage is used for focus setup, is not part of device)

[*] crphipps@aol.com; phone/fax 1-505-466-3877; http://members.aol.com/crphipps/PA/PA.html; Photonic Associates, 200A Ojo de la Vaca Road, Santa Fe NM 87508

[**] jluke@nmeri.unm.edu; phone/fax 1-505-272-7275; NMT/Institute for Engineering Research and Applications, 901 University Blvd. SE, Albuquerque, NM 87106-4339

2. OPERATING PRINCIPLES

The principle of operation is shown in Figure 1. Usually, the device is operated in Transmission mode ("T-mode") to protect optics from solid contaminants produced by the ablation jet. In this mode, a lens focuses the laser diode output on a 25-μm diameter spot on the transparent side of a specially-prepared fuel tape. Passing through the acetate substrate without damaging it, the beam heats a specially prepared absorbing coating on the opposite side of the tape to high temperature, producing a miniature ablation jet. Part of the acetate substrate is also ablated.

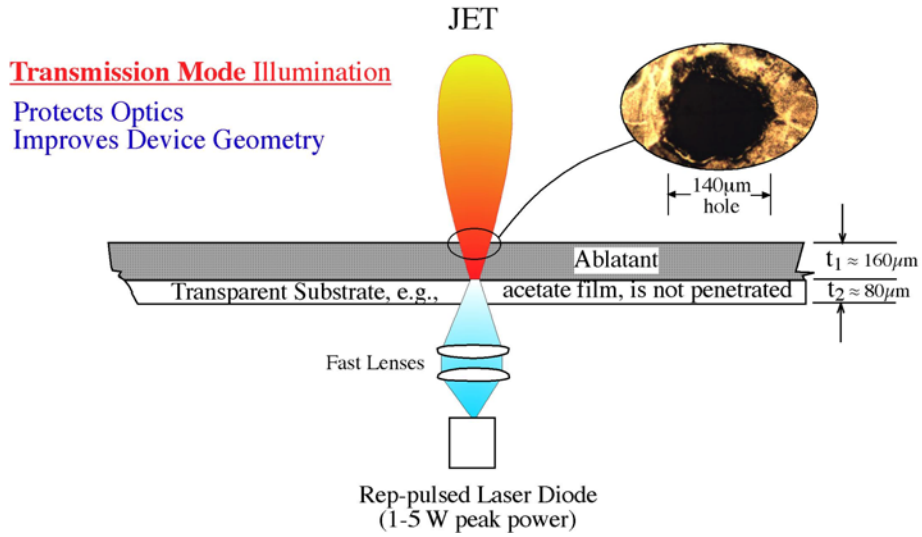

Figure 2. Target illumination arrangement for the μLPT

The μLPT can operate pulsed or CW, and power density on target is optically variable in an instant, so operating parameters can be adjusted "on the fly" to match mission requirements. Figure 3 shows the μLPT jet during normal operation.

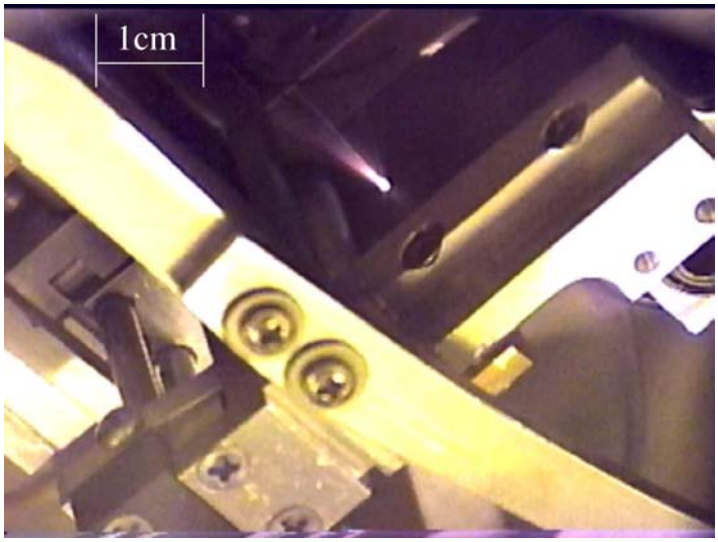

Figure 3. The μLPT in operation

Materials we have explored for the transparent substrate are cellulose acetate, PET and Kapton™ polyimide resin. For the ablatant, over 160 materials have been studied. Many of these were so-called "designer materials" created especially for this application[4-6]. One of these latter is a proprietary energetic material which has generated a laser momentum coupling coefficient (see section 5) up to 50 dyn/W, one of the highest values on record.

Using these materials, the μLPT is expected to produce 100 dyn thrust and specific impulse up to 650 s, with less than 20W electrical power input. Even with standard nonenergetic materials, specific impulse we measured was very encouraging, and exceeded values available from chemistry[2,7]. Lifetime impulse of the prototype unit, which will contain 300 g of ablator fuel, is expected to be 160 Mdyn-s. For performance of the Figure 1 preprototype, see Table 2.

3. PULSED LASER-SURFACE INTERACTIONS

Pulsed lasers offer a much rich parameter space in which to work compared to CW lasers. The latter have been well treated elsewhere[8]. For pulsed lasers, the momentum coupling coefficient C_m is defined as the ratio of target momentum $m\Delta v$ produced to incident laser pulse energy W during the ejection of laser-ablated material (the photoablation process). For continuous lasers, it is the ratio of thrust F to incident power P:

$$C_m = \frac{m\Delta v}{W} = \frac{F}{P} \tag{1}$$

In the ablation process, Q* joules of laser light (the asterisk is customary notation: Q* is not a complex number) are consumed to ablate each gram of target material:

$$Q^* = \frac{W}{\Delta m} \tag{2}$$

For the sake of discussion, we will consider a monoenergetic exhaust stream with velocity v_E. Momentum conservation requires

$$m\Delta v = \Delta m v_E , \tag{3}$$

so the product of C_m and Q* is the effective exhaust velocity v_E of the ablation stream, independent of the efficiency with which laser energy is absorbed. This can be seen by writing:

$$C_m Q^* = \frac{(\text{dyn}-\text{s})(\text{J})}{(\text{J})(\text{g})} = \frac{(\text{kg})(\text{cm})}{(\text{kg})(\text{s})} = \text{cm/s} \tag{4}$$

If for example, a significant amount of the incident energy is absorbed as heat in the target substrate rather than producing material ejection, Q* will be higher and C_m will be proportionately lower, giving the same velocity in the end.

While it is understood that real exhaust streams have velocity distributions, we have shown[9] that the monoenergetic stream approximation will not introduce large errors [$\langle v^2\rangle/\langle v\rangle^2 \approx 1.15$] for laser-produced plasmas, and the principal points we want to make will be easier to understand using that assumption.

The specific impulse I_{sp} is simply related to the velocity v_E by the acceleration of gravity:

$$C_m Q^* = v_E = g I_{sp} \tag{5}$$

Energy conservation prevents C_m and Q* from being arbitrary. Increasing one decreases the other. Using Eqs. (3) and (4), energy conservation *in a passive absorber* requires that several constant product relationships exist:

$$2E7\ \eta_{AB} = \Delta m v_E^2/W = C_m^2 Q^* = g C_m I_{sp} = C_m v_E . \tag{6}$$

In Eq. (6), we introduce the ablation efficiency parameter, $\eta_{AB} \le 1$, the efficiency with which laser energy W is converted into exhaust kinetic energy. Choosing combinations of C_m and v_E that exceed 2 violates physics, since η_{AB} must be less than 1. [The "1E7" in Eqs. (6) and (8) following is because of the mixed practical units in which it is customary to write C_m in the laser ablation literature (dyn/W)].

Since the maximum specific impulse of ordinary chemical rockets is about 500s, limited by the temperatures available in chemical reactions, exit velocity v_E > 5km/s (I_{sp} > 5000s) is accessible only by laser ablation, where temperatures can easily be many times 10,000K, or some other non-chemical process such as ion drives. Specific impulse I_{sp} up to 8000s has been measured with pulsed lasers[10].

Ablation efficiency can approach 100%, as direct measurements with other types of lasers on cellulose nitrate in vacuum verify[10], but a value of 50% or even less is likely. The impact of η_{AB}<1 is that the C_m value deduced from a given v_E may be less than the maximum permitted by conservation of energy. Exit velocity v_E is the fundamental quantity.

The rate of mass usage is $$\dot{m} = \frac{P}{Q^*} \qquad \text{g/s} \tag{7}$$

where P is laser optical power. When considering C_m and Q* as design variables it must be kept in mind that the ablator lifetime increases with Q* and decreases very rapidly with increasing C_m:

$$\tau_{AB} = \left| M/\dot{m} \right| = \frac{MQ^*}{P} = \frac{2E7\ \eta_{AB} M}{P C_m^2} = \frac{g^2 M I_{sp}^2}{2E7\ P\ \eta_{AB}} \tag{8}$$

For this reason, in laser propulsion applications, increasing C_m to get more thrust via the relationship

$$F = PC_m \tag{9}$$

from a given laser entails a serious penalty for ablator lifetime, because $\tau_{AB} \propto 1/C_m^2$ from Eq. (8).

The vacuum coupling coefficient C_m is in the range 1 – 10 dyn/W for standard surface-absorbing materials[9].

Note that, from Eq. (6), $C_m{*}I_{sp}$ <= 2E7/g = 2.04E4. In measurements with energetic target materials, products $C_m{*}I_{sp}$ = 1.8E4 have been obtained[8], which is 90% of 2.04E4.

In the laboratory, C_m and Q* are relatively easy quantities to measure, and their product conveniently gives v_E which is a difficult quantity to measure, requiring, e.g., a laser-induced fluorescence setup or time-resolved shadowgraphy.

Vacuum plasma theory adapted from laser fusion[11,12] well describes the situation above plasma threshold, as has now been generally accepted[13,14]. The principal results of that work which we will use here is, for the laser-initiated plasma-mediated pressure on a plane surface:

Typical values of the coefficient C_m taken from the literature are shown in Table 1.

$$p_{AB} = 5.83 \frac{\Psi^{9/16}}{A^{1/8}} \frac{I^{3/4}}{(\lambda\sqrt{\tau})^{1/4}} \tag{13}$$

and

$$T_e = 2.98\text{x}10^4 \frac{A^{1/8} Z^{3/4}}{(Z+1)^{5/8}} (I\lambda\sqrt{\tau})^{1/2} \tag{14}$$

for the plasma electron temperature (K), where Ψ = the coefficient $(A/2)[Z^2(Z+1)]^{1/3}$, A is the plasma average atomic mass number and Z is the plasma average ionization state number. For coupling coefficient, Eq. 13 gives

$$C_m = 5.83 \frac{\Psi^{9/16}}{A^{1/8} (I\lambda\sqrt{\tau})^{1/4}} \tag{15}$$

Note that Eq. (15) predicts C_m becomes very large in the limit $I\lambda\sqrt{\tau} \rightarrow 0$. This may seem counterintuitive, but one has to remember that C_m is just the ratio of a momentum to an energy and so varies ~1/v, becoming very large as $v \rightarrow 0$. I_{sp} is equally important in the sense that, from Eq. (6), as C_m becomes very large, I_{sp} becomes very small, which is not desirable in all cases. That is to say, there is an optimum C_m for all missions, related to the Δv which is to be supplied.

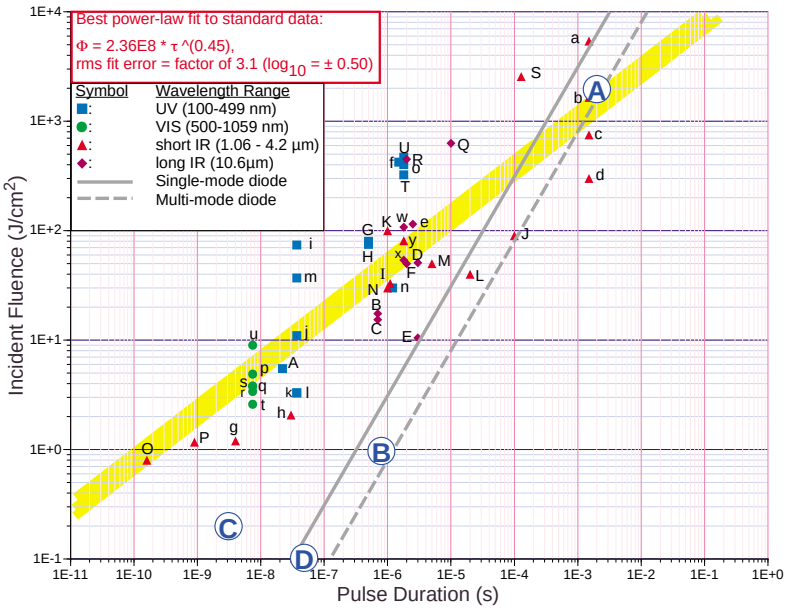

Figure 4. Fluence for plasma formation and optimum coupling vs. pulse duration from 46 data sets ranging from UV to IR wavelengths and pulse durations from 100 ps to 2 ms follow the Eq. (16) trend. Gray lines in the Figure show intensities that are accessible by common diode lasers and focusing optics. "A"–"D" refer to operating points of experiments discussed in Table 1 below. Data point labels are referenced in Phipps and Luke[2].

In addition, intensity I should be large enough to create plasma for many applications, since the vapor regime is very inefficient, producing low I_{sp} because of the low temperature, and this puts a lower limit on $I\lambda\sqrt{\tau}$. For this reason, high C_m often goes together with low I_{sp}.

The plasma to vapor transition is indicated by the broad diagonal bar across Figure 4, which shows the threshold fluence for plasma initiation and optimum coupling, based on analysis of data from 46 experiments reported in the literature[2].

This trend is

$$\Phi = b\,\tau^m \tag{16}$$

or

$$I = b\,\tau^{m-1} \tag{17}$$

with b = 2.4E4 and m = 0.45 for the

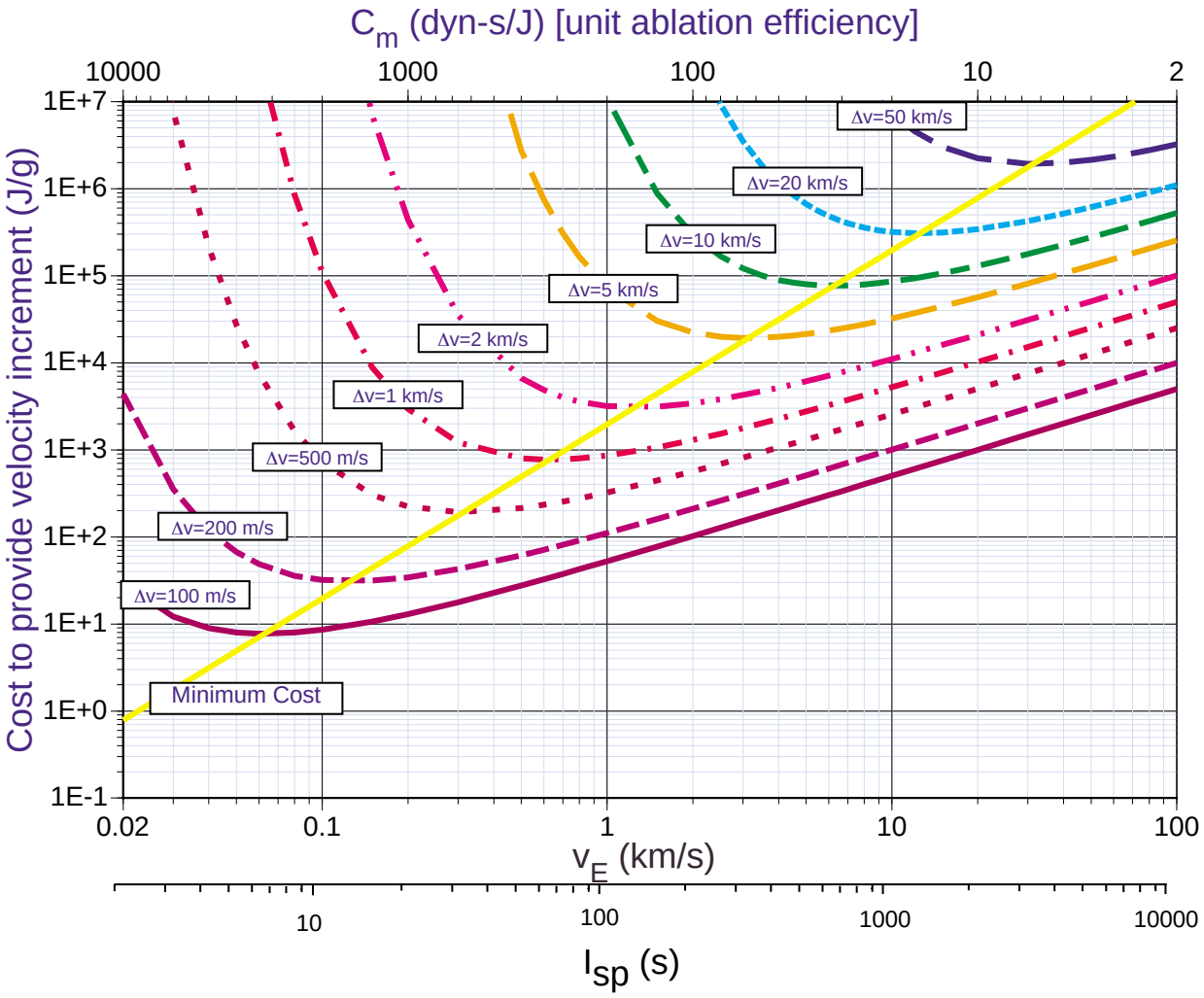

Figure 5. Energy cost (J/g) vs. exhaust velocity for a mission in vacuum with no gravity, for various values of Δv. The second (lower) horizontal axis shows corresponding values for I_{sp}, while the third (upper) horizontal axis shows corresponding, inversely varying values of C_m, taking η_{AB}=1.

100ps to 1ms range. We would have m=0.50 if the threshold for plasma formation and optimum coupling were governed by purely thermal considerations.

The optimum C_m for a given mission is related to the Δv for that mission. Figure 5 illustrates this dependence.

In vacuum, ignoring gravity, the energy cost C is given by the expression[9]

$$C = \frac{v_E^2}{2E7}\,[\exp(\Delta v / v_E) - 1] \qquad (18)$$

while the optimum (minimum) cost is given by[13]

$$\frac{\Delta v}{v_E} = 1.5936 \qquad (19)$$

so that the minimum cost trend in Fig. 5 is

$$C = 1.96E\text{-}7\ v_E^2\ . \qquad (20)$$

In turn[9],

$$v_E = g I_{sp} \approx v_{thi} = \sqrt{2kT_i / m_i} = 9.83E5 \sqrt{T_{i(eV)} / M_A}\ . \qquad (21)$$

In short, large C_m and low I_{sp} is a good trade only for low velocity missions. When C_m is unduly high, a lot of thrust is generated per unit of laser power, but the low I_{sp} means that the fuel is depleted before the mission can be

completed [see Eq. (8)]. Vice versa, an engine with unduly high I_{sp} preserves the fuel indefinitely, but has no thrust.

Table 1 gives a cursory summary of the range of values that are found for C_m, as well several other parameters. Even though I_{sp} was not measured in all cases, it can be deduced from the experimental variables. It can be seen that I_{sp} drops precipitously as the Table is descended, as do ion temperature T_i, exhaust velocity and I_{sp} [refer to cases "A"–"D" in Figure 4].

Table 1. Summary of C_m literature
"A" – "D" refer to points indicated on Figure 4

Reference	**Target**	**Laser λ,τ**	**Min. Laser Φ** (J/cm^2)	**Max. C_m** (dyn/W)	**Max. I_{sp}** (s) [upper bound from Eq. 6]	**Min. Product $I\lambda\sqrt{\tau}$** ($W\sqrt{s}/cm$)
11	Simple passive (front illuminated)	various	various	10	----	0.5
This work	Proprietary energetic absorber	970 nm, 2ms	2E3 "A"	52	550	4
15	Energetic absorber pyroxylin (front illuminated)	10.6 μm, 2μs	5E6	95	200	8
16	Confined passive absorber	1.06 μm, 85ns	1 "B"	492	1.0	0.4
14	Confined passive absorber	1.06μm, 3ns	0.2 "C"	700	[≤ 29]	0.3
17	Simulation of front-illuminated target in low-fluence limit	1.06μm, 50ns	0.1 "D"	6000	[≤ 3.4]	0.05

4. INDUCING SHOCK IN TARGETS

Whether or not a shock is formed is an important consideration when planning to illuminate an energetic target material, to determine whether a laser-supported detonation will propagate.

The classic analysis of high-intensity laser interaction with materials divides into two regimes: laser supported combustion (LSC) and laser supported detonation (LSD)[18-20]. Although the analysis was originally developed by aerodynamicists for interactions in air, these concepts can also apply to a solid target in vacuum. The transition from the LSC to LSD regime is caused by laser intensity sufficient to produce a shock wave in the material, i.e., wave velocity greater than the particle thermal velocity.

For our purposes, it is sufficiently accurate to describe shock formation by the relationship

$$\nabla p = \rho v \cdot \nabla v \quad , \tag{22}$$

from which

$$p = \rho v^2 = \rho c_s^2 \quad . \tag{23}$$

Taking sound speed c_S=1E5 cm/s and mass density ρ=1 g/cm^3 we find laser-induced pressure $p \cong$ 1E10 dyn/cm^2 = 10 kbar is necessary to produce a shock.

The energy density involved is:

$$u = \frac{3}{2}nkT = \frac{3}{2}p = \frac{3}{2}(1E10)\ erg/cm^3 \tag{24}$$

Or, in practical terms, u = 1500 J/cm^3.

Eq. (13) gives the combination of laser intensity I (W/cm^2), pulsewidth τ (s) and wavelength λ(cm) will give the required 10kbar pressure. Without much loss, we can take Ψ=1 and, for a carbon-hydrogen plasma, A=6 in Eqs. (13) and (14).

Table 2 uses these values to illustrate the order of magnitude of pressure predicted by Eq. (13) during a laser pulse which is front-illuminating a standard-material target in vacuum at λ=970nm.

Table 2. Laser-induced pressure vs. laser parameters

Pulse duration	Conditions	Intensity I	Pulse energy W	Pressure (bar)
4ms	μLPT parameters	13 kW/cm^2	4 mJ	0.43
10 ns	Laser fusion	5.9 GW/cm^2	1800 J	10k

In other words, it requires laser fusion conditions in an unconfined target to create a propagating detonation in the target. In a confined target, on the other hand, it takes far less laser intensity. Fabbro, *et al* . have shown[14] pressure amplification up to a factor of 70 by confining the plasma between an anvil and a glass plate through which the laser light is introduced to the target. Other workers have replaced the glass plate with a liquid film for industrial applications[21]. Nevertheless, for pulse durations we plan for the μLPT, shock formation is highly unlikely.

5. PROGRESS WITH THE PREPROTOTYPE THRUSTER

5.1 Operating Parameters

Since our previous report on this work[22], considerable progress has occurred. Table 3 shows the parameters for the "preprototype" microthruster that we have developed, including expected behavior when the energetic fuel tapes are used. We determine thrust in vacuum with a torsion balance[2] which can measure 5 dyn with 10% accuracy. Its force response is 500 dyn/rad.

Table 3. Expectations for the μLPT preprototype

Parameter	**Value ± 10% unless noted**
Weight with fuel	850 g
Tape dimensions	50.5cm x 2.54cm x 240 um
Laser wavelength	970 nm
Laser power (average, peak)¶	2 W, 10W
Laser focal distribution dims	25 μm dia.
Tape speed	10 mm/s
Pulse duration τ	4 ms
Duty factor	0.2
Pulse repetition frequency	40 Hz
Track width, normal operation	100μm
Tracks	254
Nominal tape lifetime	3.5 hours
Coupling coefficient C_m	50 dyn/W
Typical fluence on target Φ	2000 J/cm^2
Force output §	100 dyn
Lifetime impulse J_{tot}	1.3 Mdyn-s
Q*	11 kJ/g
I_{sp}	400 s
Minimum impulse bit	0.1 dyn-s†
Maximum laser heatsink temperature	80C

§: with energetic ablatant; ¶: when fiber-coupled diode lasers are installed; †: at 1ms pulsewidth

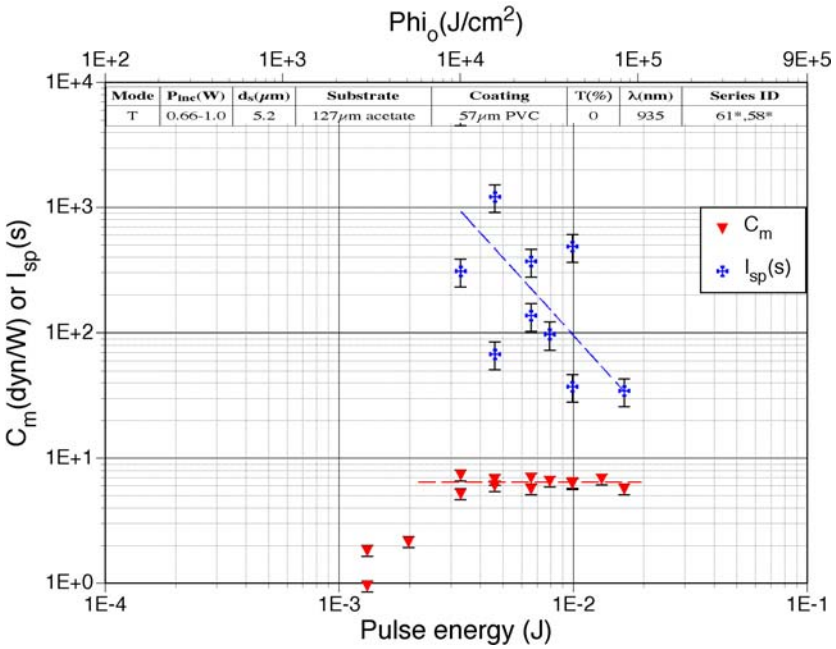

Figure 6. Coupling coefficient and specific impulse measured with single pulses from the single-mode research laser focused to 5μm spot diameter, on standard PVC/Acetate target material in T mode. Note the nearly constant C_m value of 6.2 dyn/W (62 N/MW) above threshold. For the upper horizontal axis, 100J/cm^2=1MJ/m^2. Specific impulse I_{sp} in excess of 1000 s was seen.

Control of, and communications with, the thruster in the vacuum chamber is achieved via a universal asynchronous receiver transmitter channel and an onboard Texas Instrument MSP430 microcontroller. The MSP430 was chosen for its ultra low power, only 7 mW at full computing speed and only 5μW in standby. Total mass for the microcontroller and ancillary electronics is about 2.2 grams.

5.2 Static Test Data

Figure 6 shows typical results we have obtained in static (single-pulse) tests designed to identify likely target materials for our μLPT.

Figure 7 shows the very encouraging recent static test results we obtained with a proprietary energetic material, which is the basis for the thrust quoted in Table 3.

5.3 μLPT Operation

We have made tapes from several of the ablatant/substrate combinations identified in the static impulse tests and tested their performance using the "preprototype" continuous thrust test device.

To measure thrust, we use a sensitive, μN torsion pendulum which suspends the thruster and its electronics.[2] The pendulum is calibrated using pair of magnetic coils. A large field coil is attached to the support frame, and a small armature coil is attached to the pendulum, which is oriented perpendicular to the field coil. By applying current to the coils, a small well-defined torque can be applied to the pendulum and its response measured. The field coil produces a magnetic field much larger than the local horizontal component of the Earth's field.

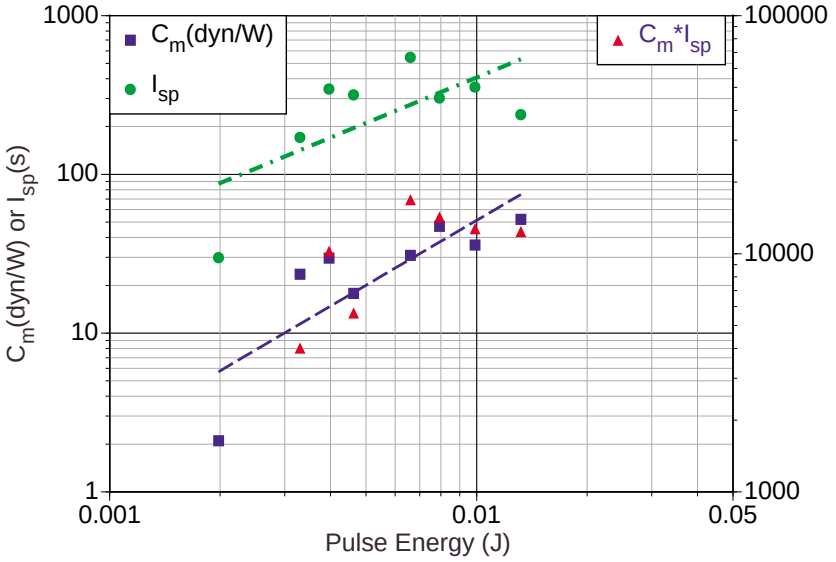

Figure 7. C_m as large as 50 dyn/W (500 μN/W) and I_{sp} up to 550s were obtained with proprietary energetic μLPT fuel. Maximum product C_m*I_{sp} = 16,870, a figure which is equivalent to 83% of the theoretical maximum for a perfectly efficient *nonenergetic* absorber.

We always operate the μLPT preprototype in repetitively-pulsed mode, because we found that the moving tape steers the μLPT jet unacceptably in CW mode[3]. During a ms-duration pulse, however, tape motion is negligible and the plume is well-defined [Figure 3] and perpendicular to the tape. This change brought with it three benefits: operation in closer

contact with the bulk of our experimental data (which is pulsed data), operation at higher peak power for better I_{sp}, and low duty factor operation of our laser diodes, which is better for heat dissipation. It also brought a difficulty: the low duty factor requires us to use more diodes for the same average power and thrust. The requirement for pulsed power will have only a minor impact on the weight of the microthruster unit.

The combination of Φ and τ we use in the preprototype puts us well into the plasma regime (point "A", Figure 4).

Figure 8 shows preliminary measurements of thrust using standard (non-energetic) target materials at low laser power. These results meet Air Force thrust requirements for TechSat21-type missions. Much larger I_{sp} will be seen in full power tests now being implemented with new diodes which will achieve a 3-fold increase in optical power.

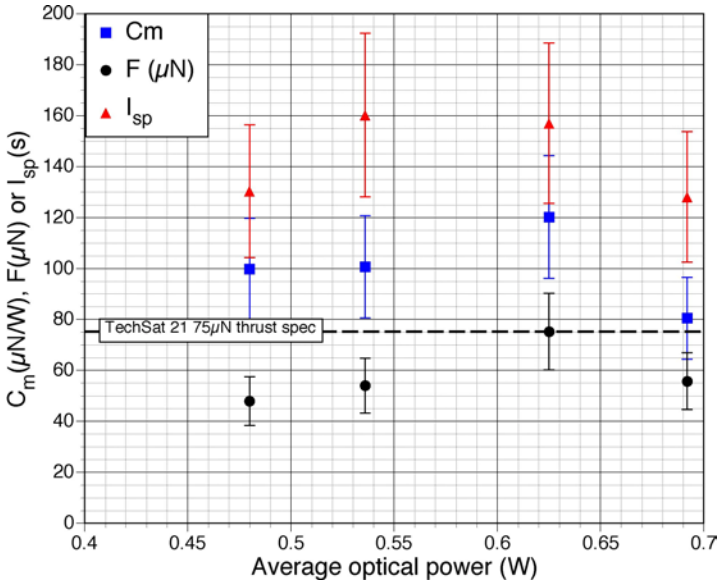

Figure 8. First measurements of thrust, thrust-to-power ratio and specific impulse for the preprototype in low-power tests.

For these tests, four JDSU 6380-A fiber-coupled, 920-nm diodes [Figure 9] deliver 15W peak power (3W average) to the target in a tightly focused spot. For the Figure 8 data, only 30% of this power was available.

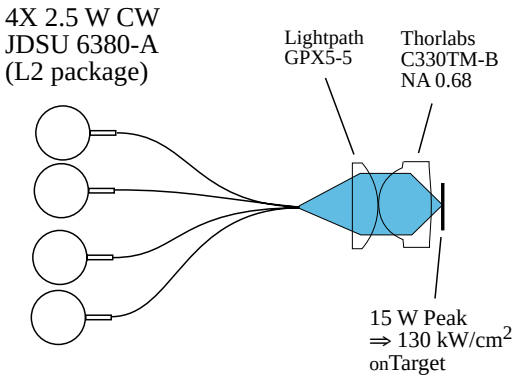

Figure 9. High power laser illumination scheme images optical fibers on target at high peak power.

Prototype

The μLPT prototype thruster will incorporate advances in performance developed with the preprototype and, instead of 50cm of fuel tape, will incorporate 400g of expendable fuel in an 80-m x 2.54-cm tape, enabling it to generate an impulse of 2500 N-s over its 750-hour lifetime. This is sufficient to de-orbit or significantly raise the orbit of a microsatellite, in addition to the primary function of attitude control for which the μLPT is designed.

6. SUMMARY

A new type of microthruster has been developed which is an alternative to the μPPT for spacecraft microthrusters. The μLPT is one of the first practical application of laser ablation propulsion. When complete, the μLPT prototype will exceed all Air Force requirements for TechSat21-type microthrusters.

Laser-surface interaction theory shows that the combination of coupling coefficient C_m and specific impulse I_{sp} developed by this thruster are appropriate for its mission.

ACKNOWLEDGMENT

This work was completed with support from AFOSR contract F49620-00-C-0005

REFERENCES

1. A. Kantrowitz, *Aeronaut. Astronaut.* **10**, 74 (1972)

2. C. Phipps and J. Luke, "Diode Laser-driven Microthrusters: A new departure for micropropulsion," *AIAA Journal* **40** (2) pp. 310-318 (2002)

3. J. Luke, C. Phipps and G. McDuff, "Laser Plasma Thruster Continuous Thrust Experiment", paper 4760-105, this

conference.

4. T. Lippert, C. David, M. Hauer, A. Wokaun, J. Robert, O. Nuyken, C.R. Phipps, S. Langford, J. Dickinson and U. Kogelschatz, “Structure Property Relations of Photoreactive Polymers Designed for Laser Ablation”, *J. PCB* (2001)

5. T. Lippert, C. David, M. Hauer, T. Masubuchi, H. Masuhara, O. Nuyken, C. Phipps, J. Robert, T. Tada, K. Tomita, A. Wokaun, Novel applications for laser ablation of photopolymers, invited paper for special issue of *Appl. Surf. Sci.*, in preparation (2002)

6. T. Lippert, C. David, M. Hauer, C. Phipps, A. Wokaun, Tailor-Made Polymers for Laser Applications, [invited paper for special issue] *Review of Laser Engineering*, **29**, no. 11, pp 734-738 (2001)

7. C. Phipps, J. Luke and G. McDuff, "A diode-laser-driven microthruster", *Proc. International Electric Propulsion Conference, Pasadena*, paper IEPC-01-220 (2001)

8. P. Loosen, "Advances in CO_2 laser technology for industrial applications", SPIE **1810** pp. 26-33 (1993)

9. C. Phipps, J. Reilly and J. Campbell, “Optimum Parameters for Laser-launching Objects into Low Earth Orbit”, J. *Laser and Particle Beams*, **18** no. 4 pp. 661-695 (2000)

10. C. Phipps and M. Michaelis, “Laser Impulse Space Propulsion”, *Journal of. Laser and Particle Beams* vol.12 no. 1, pp. 23-54 (1994)

11. C. Phipps, T. Turner, R. Harrison, G. York, W. Osborne, G. Anderson, X. Corlis, L. Haynes, H. Steele, K. Spicochi, and T. King, "Impulse Coupling to Targets in Vacuum by KrF, HF and CO_2 Lasers" , *Journal of. Applied. Physics.*, vol. 64, no. 3 pp. 1083-96 (1988)

12. C. Phipps and R. Dreyfus, "Laser ablation and plasma formation" in *Laser Ionization Mass Analysis,* Akos Vertes, Renaat Gijbels and Fred Adams, eds., Wiley, New York, May, (1993)

13. A. Saleres, *et al.,* “Couplage thermique et mécanique dans l’interaction laser-matière a éclairement modéré”, *Revue Scientifique et Technique de la Defense*, CEL-Valenton report 77 (1992)

13. W. Möckel, "Optimum Exhaust Velocity for Laser-Driven Rockets", J. *Spacecraft and Rockets* **12**, p. 700-1 (1975)

14. R. Fabbro, J. Fournier, P. Ballard, D. Devaux and J. Virmont, “Physical study of laser-produced plasmas in confined geometry”, *J. Appl. Phys.* **68**, pp. 775-784 (1990)

15. C. Phipps, Jr., R. Harrison, T. Shimada, G. York, T. Turner, X. Corlis, H. Steele, L. Haynes and T. King, "Enhanced Vacuum Laser-impulse Coupling by Volume Absorption at Infrared Wavelengths", *Laser and Particle Beams*, **8**, 281 (1990)

16. C. Phipps, D. Seibert II, R. Royse, G. King and J. Campbell, “Very High Coupling Coefficients at Low Laser Fluence with a Structured Target,” Proc. Santa Fe High Power Laser Ablation Conference, April 23-28, 2000, SPIE **4065** pp. 931-7 (2000)

17. T.Yabe, C.Phipps, K.Aoki, M.Yamaguchi, R.Nakagawa , H.Mine , Y.Ogata , C. Baasandash, M.Nakagawa, E.Fujiwara, K.Yoshida , A.Nishiguchi and I.Kajiwara, " Micro-airplane Propelled by Laser-Driven Exotic Target", *Applied Physics Letters*, to appear (2002)

18. A. Pirri, "Theory for momentum transfer to a surface with a high-power laser", Phys. Fluids vol. 16, pp. 1435-1440 (1973)

19. A. Pirri, R. Root and P. Wu, "Plasma energy transfer to metal surfaces irradiated by pulsed lasers", *AIAA Journal*, **16**, pp. 1296-1304 (1978)

20. Yu. Raizer, *Laser-induced Discharge Phenomena*, Consultants Bureau, New York (1977) pp. 198-249

21. P. Peyre, R. Fabbro, L. Berthe, X. Scherpereel and E. Bartnicki, "Laser shock processing of materials and related measurements", SPIE **3343** pp. 183-193 (1998)

22. C. Phipps and J. Luke, "Micro Laser Plasma Thrusters for Small Satellites", SPIE **4065**, pp 801-809 (2000)